CERN-INTC-2015-012 / INTC-P-317-ADD-2
14/01/2015

EUROPEAN ORGANIZATION FOR NUCLEAR RESEARCH

Addendum to the ISOLDE and Neutron Time-of-Flight Committee

IS532: Mass spectrometry of neutron-rich nuclides into the $N = 40$ "island of inversion"

January 14, 2015

N. Althubiti[1], P. Ascher[2], D. Atanasov[3], D. Beck[4], K. Blaum[3], M. Breitenfeldt[5,6], R. B. Cakirli[7], T. E. Cocolios[1], S. Eliseev[3],T. Eronen[8], S. George[3], F. Herfurth[4], A. Herlert[9], M. Kowalska[6], S. Kreim[3,6], Yu. A. Litvinov[4], D. Lunney[10], V. Manea[3], E. Minaya Ramirez[3], S. Naimi[11], D. Neidherr[4], M. Rosenbusch[12], A. de Roubin[3], L. Schweikhard[12], A. Welker[13], F. Wienholtz[12], R. N. Wolf[3], K. Zuber[13]

[1] *The University of Manchester, Manchester, United Kingdom*
[2] *Centre d'Etudes Nucléaires de Bordeaux-Gradignan, France*
[3] *Max Planck Institute for Nuclear Physics, Heidelberg, Germany*
[4] *GSI Helmholtzzentrum für Schwerionenforschung GmbH, Darmstadt, Germany*
[5] *Grupo de Fisica Nuclear, Universidad Complutense, Madrid, Spain*
[6] *CERN, Geneva, Switzerland*
[7] *Istanbul University, Department of Physics, Istanbul, Turkey*
[8] *University of Jyväskilä, Jyväskilä, Finland*
[9] *FAIR GmbH, Darmstadt, Germany*
[10] *CSNSM-IN2P3-CNRS, Université Paris-Sud, Orsay, France*
[11] *RIKEN, Wako, Saitama, Japan*
[12] *Ernst-Moritz-Arndt-University, Greifswald, Germany*
[13] *Technical University, Dresden, Germany*

Spokesperson: Susanne Kreim, skreim@cern.ch
Contact person: Vladimir Manea, vladimir.manea@cern.ch

Abstract:

Following the recent measurement of the energy of the first excited 2^+ state in ^{54}Ca and the generally large interest in shell evolution in the pf valence space, lacking precise knowledge of ground-state binding energies, we propose to continue the series of IS532 mass measurements of $Z \geq 20$ nuclides with $^{60-62}$Cr and $^{\geq 55}$Ca. These new measurements would bring crucial complementary information for understanding nuclear-structure evolution between ^{52,54}Ca and ^{68}Ni, all considered closed-shell, through a region of increase collectivity, in which the $N = 40$ harmonic-oscillator shell closure breaks down. This addendum would benefit from the recent availability of neutron-rich chromium beams at ISOLDE, as well as already existing ISOLTRAP measurements of chromium isotopes up to $A = 59$ and calcium isotopes up to $A = 54$.

Requested shifts: 9 shifts of chromium beams in one run and 6 shifts of calcium beams in one run

1 Motivation

Nuclear shell effects continue to be a research topic of great interest more than half a century after the first microscopic nuclear model [1,2]. Closed-shell nuclei (otherwise known as "magic") exhibit increased stability in the ground state and are more difficult to excite, which is usually characterized by a high energy of the first 2^+ excited state $E(2_1^+)$ and a low reduced quadrupole transition probability $B(E2; 2_1^+ \rightarrow 0_1^+)$ (in W. u). With the advances of experimental techniques for the production and study of radioactive ion beams, closed-shell nuclei have been systematically investigated to verify the robustness of shell closures against neutron excess or deficiency. Although generally understandable considering that the nuclear mean field changes with the addition or removal of a single nucleon, this type of research has found a rather intuitive framework with developments in the modeling of the residual nucleon-nucleon interaction. Specifically, the concept of effective single-particle energies (ESPE) offered an intuitive way to quantify the (effective) size of an energy gap in the single-particle spectrum, while the monopole part of the residual interaction was identified as the driving force in the evolution of ESPE [3]. The study of closed shells and their evolution with neutron-to-proton asymmetry can thus directly contribute to constraining the properties of the residual interaction in shell-model studies. The tensor part of exclusively two-body effective interactions and the three-body part of interactions derived in chiral effective field theory were identified as particularly important ingredients influencing the emergence or disappearance of shell closures across the nuclear chart (see [4] and [5] for recent related examples).

Perhaps the best known example of what is now called "shell evolution" is that of the $N = 20$ harmonic-oscillator magic number, where the reduction of the energy gap between the $\nu d_{3/2}$ and $\nu f_{7/2}$ levels (above the $N = 20$ shell), together with the proximity of the quadrupole partners $\nu f_{7/2}$ and $\nu p_{3/2}$, drives the deformation of the $N = 20$ isotones for $Z < 20$ [6] and leads to the so-called "island of inversion" in the *sd* shell. A similar situation seems to be true for the next harmonic-oscillator magic number $N = 40$. Although already at the mean-field level the $N = 40$ gap is diminished by the spin-orbit interaction, making it rather a pronounced subshell, its evolution for $Z < 28$ follows closely the one observed for $N = 20$. Thus, while $^{68}_{28}$Ni exhibits the properties of a doubly-magic nucleus, the reduction of the energy gap between the $\nu f_{5/2}$ and $\nu g_{9/2}$ (above $N = 40$), together with the proximity of the quadrupole partners $\nu g_{9/2}$ and $\nu d_{5/2}$, quickly drives the collectivity of the $N = 40$ isotones with $Z < 28$, making some authors call this region of the *pf* shell another island of inversion [6].

Recent experimental studies confirm this view and show the *pf* shell to be a quite complex valence space for studying shell evolution. Measurements of the $E(2_1^+)$ values in ^{52}Ca [7] and ^{54}Ca [4] hint at the closure of the $N = 32$ and $N = 34$ sub-shells for $Z = 20$, the former confirmed by mass measurements with ISOLTRAP [5] performed as part of the IS532 experiment. Mass measurements of calcium isotopes beyond $N = 34$ are thus of great interest, because they would allow determining the $N = 34$ shell gap and confront state-of-the-art shell model calculations, which as shown in [4,5] differ greatly at $N = 34$. For $Z = 28$ the situation seems quite different. No particular enhancement of $E(2_1^+)$ is observed at $N = 32$ and $N = 34$, but a pronounced local maximum emerges at $N = 40$, hinting at another sub-shell effect [8]. In between, measurements of $E(2_1^+)$ [9–11] and recently $B(E2; 2_1^+ \rightarrow 0_1^+)$ [12–15] values of iron and chromium isotopes show that removing only two protons from the $Z = 28$ core is enough to weaken the $N = 40$ closure. Theoretical attempts to reproduce this rapid evolution in shell model revealed the necessity of going beyond the *pf* shell. GXPF1A calculations in the *pf* space, not including the $\nu g_{9/2}$, fail to reproduce the levels in ^{60}Cr [16]. Allowing excitations above the $N = 40$ gap to $\nu g_{9/2}$ produces a change in the right direction [17], but as shown in [6] the occupation of the $\nu d_{5/2}$

orbital can be significant, requiring a full $pfgd$ treatment. The important role of the $\nu g_{9/2}$ and $\nu d_{5/2}$ orbitals for the development of collectivity at $N = 40$ is also clearly shown in a recent systematic study [18], where the simple pfg treatment fails to reproduce even the basic trends for $N \geq 38$. Interestingly, the $\nu d_{5/2}$ orbital is shown in [18] to be less relevant for the nickel and calcium chains, but very important for the description of the mid proton-shell nuclei (e.g. chromium). Mid-shell nuclei in the $N \approx 40$ region are thus complementary to the magic ones in testing the different aspects of theoretical models.

The maximum collectivity is found in the chromium isotopic chain, with quadrupole deformation estimated from $B(E2\uparrow)$ at $\beta_2 \approx 0.3$ [19]. This convinced some authors to speak of a new region of deformation [6, 10], however total Routhian surface calculations point to a rather soft intrinsic shape in the γ degree of freedom [16], with a shallow minimum close to the spherical shape. Projected shell model calculations based on a microscopic-macroscopic approach [20] support this latter view, emphasizing the role of multiparticle-multihole configurations and shape mixing to describe the chromium nuclei. Beyond-mean-field calculations based on the Gogny-D1S interaction with configuration mixing describe the general trend of $E(2_1^+)$ values along the iron isotopic chain, but systematically overestimate them [12], while the D1S potential energy surfaces show indeed no pronounced deformed minimum, but rather a flat landscape around the spherical shape [21].

To elucidate the structure of $Z < 28$, $N \approx 40$ nuclei, ground-state properties are required, especially binding energies which, studied along an isotopic chain, can trace the evolution of the ground-state correlation energy and be compared to model predictions. Nucleon separation energies can be very sensitive to the onset of deformation, either by sudden jumps or deviations from a linear trend, as can be observed for the neutron-rich $A \approx 100$ nuclides [22].

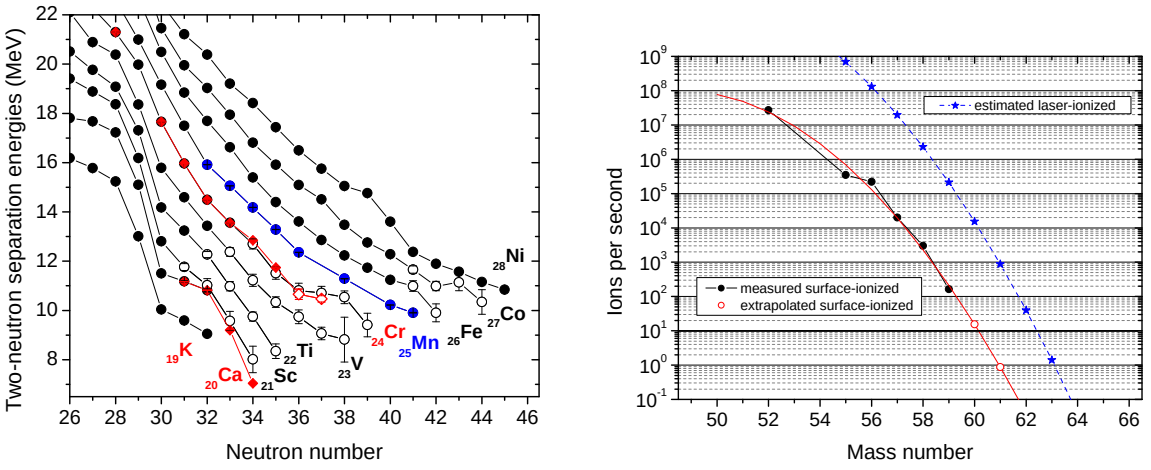

(a) (b)

Figure 1: (a): Two-neutron separation energies in the region of interest. The values obtained using masses from AME2012 [22] are marked by circles. Open circles mark data points determined from low-precision measurements [23–27]. The blue symbols mark the data from [28]. Values using recent ISOLTRAP mass measurements are given in red diamonds, namely calcium masses published in [5] and chromium masses up to ^{59}Cr measured opportunistically in 2014 (the open diamonds represent data points for which only one of the involved masses was determined by ISOLTRAP). The S_{2n} values obtained using the ISOLTRAP masses of ^{52,53}K [29] are not shown. (b): Yields of neutron-rich chromium isotopes estimated in 2014 by ISOLTRAP. The surface-ionized yields directly measured are marked by black circles, the yields with laser ionization, assuming a factor 10^3 enhancement, are given in blue stars.

Figure 1(a) shows the current knowledge of two-neutron separation energies (S_{2n}) in the region of interest, using data from the atomic mass evaluation [22], recent ISOLTRAP masses of calcium isotopes [5] and preliminary masses of chromium isotopes up to $N = 35$ measured in 2014 at ISOLTRAP (the latter two in red diamonds). ISOLTRAP has also determined the masses of ^{52,53}K, recently submitted for publication but not shown in the figure [29]. An important part of the masses in the region were determined with low precision in a series of measurements by the TOFI spectrometer at Los Alamos [23–25], FRS-ESR at GSI [26] and TOF technique at NCSL [27]. The data points which still rely mainly on these measurements in the evaluation are marked by open symbols. Since then, many of the masses for $Z > 24$ have been determined by Penning-trap mass spectrometry: nickel masses by ISOLTRAP [30] and JYFLTRAP [31], cobalt and iron masses by LEBIT [32, 33] and manganese masses by ISOLTRAP [28] (marked in blue). In the chromium isotopic chain, so far only ^{56,57}Cr were measured by ISOLTRAP [34]. The S_{2n} values of iron and manganese isotopes start to gradually curve up beyond $N = 36$. In [28] an actual kink in S_{2n} is presented, however it is not clear whether the $N = 37$ manganese mass belongs to the ground state or to a long-lived isomer (hence the missing data points in Fig. 1(a)). Along the chromium isotopic chain the effect should be maximal and the S_{2n} values obtained from low-precision measurements show an important kink at $N = 37$. However, mass measurements of chromium isotopes performed with ISOLTRAP in 2014 (up to $N = 35$) found deviations at $N = 34, 35$, which call for a measurement of the more neutron-rich isotopes with higher precision. Such measurements would also allow determining the two-neutron gap at $N = 34$.

2 Experimental setup

The current addendum concerns the Penning-trap mass spectrometer ISOLTRAP [35], which now comprises a linear, radio-frequency quadrupole cooler and buncher (RFQ), a multi-reflection time-of-flight mass spectrometer (MR-TOF MS) and two Penning traps, one for preparation and one for precision mass spectrometry (see [36] for the most recent update on the ISOLTRAP setup). The MR-TOF MS has become routinely used at ISOLTRAP either as a beam purifier [37] or beam analyzer [38], the latter application producing also the first mass measurements of calcium isotopes in the framework of the IS532 experiment [5]. ISOLTRAP possesses now two independent methods for mass determination. For yields as low as 10^2 ion per μC and half-lives larger than 100 ms, traditional Penning-trap mass spectrometry can be applied, while the MR-TOF MS acts as a fast beam purifier. For half-lives of a few hundred ms, multiple accumulations in the preparation Penning trap of MR-TOF-purified ion ensembles (stacking) can be applied, allowing to cope with higher contamination ratios [39]. In all these cases, the MR-TOF MS can be used with little additional experimental time to perform cross-check mass measurements, which are also a means of recording the beam composition. For ions of half-life in the 10-100 ms range and yield below 10 ions per μC, the MR-TOF MS becomes the mass measurement tool, as shown by the successful measurements of ^{54}Ca [5] and ^{53}K [29]. The precision achievable with the MR-TOF MS in the $A \approx 50$ region is better than 10^{-6}.

3 Beam-time request

Neutron-rich chromium isotopes

We propose to measure the masses of $^{60-62}$Cr with the Penning-trap mass spectrometer

ISOLTRAP. We note that the $^{58-60}$Cr were requested as part of the original IS532 proposal, but the request was put on hold, requiring beam development [40]. In the meantime a new ionization scheme for chromium has been developed and tested by the RILIS team [41]. In the 2014 experimental campaign, ISOLTRAP attempted to measure neutron-rich scandium isotopes as part of the IS532 program, using an uranium carbide target, without observing any scandium beam (stable or radioactive). In the absence of scandium, the allocated shifts were used to perform yield determinations and mass measurements of surface-ionized chromium isotopes up to ^{59}Cr, as well as to set-up RILIS on the new chromium ionization scheme.
The (order-of-magnitude) estimated yields, obtained using the MR-TOF MS of ISOLTRAP, are presented in Fig. 1(b). Following the set-up of RILIS, a test of the laser enhancement of the chromium the yield was performed with ^{52}Cr, showing an enhancement by a factor greater than 800 [41]. A breakdown of the tantalum cavity of the target unit occurred before the laser enhancement could be tested using the MR-TOF MS. Still, the laser ionization efficiency was enough to allow measuring ^{59}Cr. The estimated yield which resulted is also shown in Fig. 1(b). Figure 1(b) shows an extrapolation of the measured surface-ionized chromium yields. An estimate of the expected yield with laser ionization, taking an enhancement of 10^3, is also shown. Although the yield extrapolation does not consider the drop in chromium half-life and the unknown chromium release, a measurement of ^{62}Cr is feasible, which would already be sufficient to observe the evolution of two-neutron separation energies into the region of maximum collectivity.

Neutron-rich calcium isotopes

The yield of laser-ionized ^{54}Ca estimated using the MR-TOF MS of ISOLTRAP in 2012 was on the order of 10 ions per μC, with an order of magnitude drop from ^{53}Ca. The half-life of ^{55}Ca is, at 22(2) ms [42], roughly four times lower than the half-life of ^{54}Ca. Although by extrapolation the yield is expected to be lower than 1 ion per μC, it is still in the range in which an MR-TOF mass measurement might be possible. We also note that the nano-structured uranium carbide target tested in 2014 showed a promising improvement of the yields of some key nuclides, including neutron-rich calcium [43], and might bring the short-lived calcium isotopes within reach. An additional improvement could result from using ISCOOL for bunching the ISOLDE beam, the ISOLTRAP RFQ being operated in ion guide mode. The quoted transmission efficiency of ISCOOL in bunching mode, following commissioning tests, is 50 % [44], for a bunch width of a few μs, while the typical efficiency of the ISOLTRAP RFQ is a factor 5-10 lower. A reduction of the bunch width to a few hundred ns is necessary in order to achieve reasonable resolving power in a short enough time in the MR-TOF MS. This can be obtained by adjusting the potentials in the ISCOOL trapping region and the voltage gradient used for extracting the ion bunch. This was successfully applied to the ISOLTRAP RFQ, leading to more than an order of magnitude reduction in bunch width with no significant loss in transmission efficiency [37].
We would like to request a number of shifts for studying calcium isotopes beyond $N = 34$. We note that a positive identification of calcium could allow a simultaneous yield and mass determination using the MR-TOF MS, the statistical uncertainty depending on the accumulated statistics and the resolving power achieved. The obtained information might also be of interest for the approved collinear-laser-spectroscopy experiment IS529 [45]. Tests of the ISCOOL coupled to the MR-TOF MS of ISOLTRAP can be performed on HRS with stable beam.

Detailed shift request

The table below presents the detailed request of shifts of radioactive beam for the different isotopes. The number of requested shifts includes the time required for setting-up the measurement cycle of ISOLTRAP and for the identification in the precision Penning trap of reference isobars for MR-TOF mass measurements. Apart from the shifts of radioactive beam, a number of 3 shifts of stable beam on HRS would be required for testing the coupling of the MR-TOF MS to the ISCOOL (preferably before, but not together with the calcium beam time). The chromium yields are the estimated ones of Fig. 1(b).

Isotope	Half-life (ms) [42]	Yield (μC^{-1})	Target/ion source	Method	Shifts (8h)
^{60}Cr	490(10)	10^4	UC_x/RILIS	Penning trap	2
^{61}Cr	243(9)	10^3	UC_x/RILIS	Penning trap or MR-TOF MS	3
^{62}Cr	206(12)	$10^1 - 10^2$	UC_x/RILIS	MR-TOF MS	4
^{55}Ca	22(2)	$< 10^0$	UC_x/RILIS	MR-TOF MS	6
				Total shifts of radioactive beam: 15	

Summary of requested shifts: 9 shifts of neutron-rich chromium beams from a UC_x target, with laser ionization; **6 shifts** of neutron-rich calcium beams from a UC_x target with laser ionization.

References

[1] O. Haxel, J. H. D. Jensen, H. E. Suess, *Phys. Rev.* **75**, 1766 (1949).

[2] M. G. Mayer, *Phys. Rev.* **78**, 22 (1950).

[3] E. Caurier, G. Martínez-Pinedo, F. Nowacki, A. Poves, A. P. Zuker, *Rev. Mod. Phys.* **77**, 427 (2005).

[4] D. Steppenbeck, *et al.*, *Nature* **502**, 207 (2013).

[5] F. Wienholtz, *et al.*, *Nature* **498**, 346 (2013).

[6] S. M. Lenzi, F. Nowacki, A. Poves, K. Sieja, *Phys. Rev. C* **82**, 054301 (2010).

[7] A. Huck, *et al.*, *Phys. Rev. C* **31**, 2226 (1985).

[8] S. Raman, C. N. Jr., P. Tikkanen, *At. Data Nucl. Data Tables* **78**(1), 1 (2001).

[9] M. Hannawald, *et al.*, *Phys. Rev. Lett.* **82**, 1391 (1999).

[10] O. Sorlin, *et al.*, *Eur. Phys. J. A* **16**(1), 55 (2003).

[11] S. N. Liddick, *et al.*, *Phys. Rev. C* **87**, 014325 (2013).

[12] J. Ljungvall, *et al.*, *Phys. Rev. C* **81**, 061301 (2010).

[13] N. Aoi, *et al.*, *Phys. Rev. Lett.* **102**, 012502 (2009).

[14] W. Rother, *et al.*, *Phys. Rev. Lett.* **106**, 022502 (2011).

[15] H. L. Crawford, *et al.*, *Phys. Rev. Lett.* **110**, 242701 (2013).

[16] S. Zhu, *et al.*, *Phys. Rev. C* **74**, 064315 (2006).

[17] K. Kaneko, Y. Sun, M. Hasegawa, T. Mizusaki, *Phys. Rev. C* **78**, 064312 (2008).

[18] L. Coraggio, A. Covello, A. Gargano, N. Itaco, *Phys. Rev. C* **89**, 024319 (2014).

[19] B. Pritychenko, J. Choquette, M. Horoi, B. Karamy, B. Singh, *At. Data Nucl. Data Tables* **98**(4), 798 (2012).

[20] C. F. Jiao, J. C. Pei, F. R. Xu, *Phys. Rev. C* **90**, 054314 (2014).

[21] S. Hilaire, M. Girod, *Eur. Phys. J. A* **33**(2), 237 (2007).

[22] M. Wang, *et al.*, *Chinese Phys. C* **36**, 1603 (2012).

[23] X. Tu, *et al.*, *Z. Phys. A* **337**(4), 361 (1990).

[24] H. Seifert, *et al.*, *Z. Phys. A* **349**(1), 25 (1994).

[25] Y. Bai, D. J. Vieira, H. L. Seifert, J. M. Wouters, *AIP Conf. Proc.* **455**(1), 90 (1998).

[26] M. Matoš, *Isochronous Mass Measurements of Short-Lived Neutron Rich Nuclides at the FRS-ESR Facilities*, Ph.D. thesis, Justus Liebig University, Giessen (2004).

[27] A. Estradé, *et al.*, *Phys. Rev. Lett.* **107**, 172503 (2011).

[28] S. Naimi, *et al.*, *Phys. Rev. C* **86**, 014325 (2012).

[29] M. Rosenbusch, *et al.*, *Phys. Rev. Lett.* (2015), submitted.

[30] C. Guénaut, *et al.*, *Phys. Rev. C* **75**, 044303 (2007).

[31] S. Rahaman, *et al.*, *Eur. Phys. J. A* **34**(1), 5 (2007).

[32] M. Block, *et al.*, *Phys. Rev. Lett.* **100**, 132501 (2008).

[33] R. Ferrer, *et al.*, *Phys. Rev. C* **81**, 044318 (2010).

[34] C. Guénaut, *et al.*, *J. Phys. G: Nucl. Part. Phys.* **31**, S1765 (2005).

[35] M. Mukherjee, *et al.*, *Eur. Phys. J. A* **35**(1), 1 (2008).

[36] S. Kreim, *et al.*, *Nucl. Instrum. Meth. B* **317**(0), 492 (2013).

[37] R. Wolf, *et al.*, *Nucl. Instrum. Meth. A* **686**(0), 82 (2012).

[38] R. Wolf, *et al.*, *Int. J. Mass Spectrom.* **349–350**(0), 123 (2013).

[39] M. Rosenbusch, *et al.*, *Appl. Phys. B* **114**(1-2), 147 (2014).

[40] 'Minutes of the 41^{st} meeting of the isolde and neutron time-of-flight experiments committee', CERN-INTC-2011-058, INTC-041 (2011).

[41] T. Day Goodacre, private communication (2014).

[42] G. Audi, *et al.*, *Chinese Phys. C* **36**(12), 1157 (2012).

[43] T. Stora, private communication (2014).

[44] H. Frånberg, *et al.*, *Nucl. Instrum. Meth. B* **266**(19–20), 4502 (2008).

[45] M. Bissell, *et al.*, 'Spins, moments, and charge radii beyond ^{48}Ca', CERN-INTC-2014-022 / INTC-P-313-ADD-1 (2014).

Appendix

DESCRIPTION OF THE PROPOSED EXPERIMENT

The experimental setup comprises: ISOLDE central beam line and ISOLTRAP setup. The ISOLTRAP setup has safety clearance, the memorandum document 1242456 ver.1 "Safety clearance for the operation of the ISOLTRAP experiment" by HSE Unit is released and can be found via the following link: https://edms.cern.ch/document/1242456/1.

Part of the	Availability	Design and manufacturing
ISOLTRAP setup	☒ Existing	☒ To be used without any modification